千葉大学学位申請論文

Molecular evolution of the hypervariable region of the attachment glycoprotein gene in human respiratory syncytial virus subgroup B genotypes BA9 and BA10

(HRSV-B 遺伝子型 BA9 および BA10 の *G* 遺伝子超可変領域における分子進化の検討)

千葉大学大学院医学薬学府
先端医学薬学専攻　小児病態学
(主任: 下条 直樹　教授)
長澤耕男

Abstract

We studied the molecular evolution of the C-terminal 3rd hypervariable region in the attachment glycoprotein gene of human respiratory syncytial virus subgroup B (HRSV-B) genotypes BA9 and BA10. We performed time-scaled phylogenetic analyses using Bayesian Markov chain Monte Carlo methods. We also performed a genetic distance analysis (*p*-distance analysis), positive and negative selection analyses, and a Bayesian skyline plot (BSP) analysis. We found that genotype BA9 diverged from the common ancestor of genotypes BA7, BA8, and BA10, while genotype BA10 diverged from the ancestor of genotypes BA7 and BA8. Strains of both genotypes were distributed worldwide. BA9 and BA10 diverged between 1999 and 2001. Both BA9 and BA10 evolved rapidly (about 4.8×10^{-3} substitutions/site/year) and formed three distinct lineages in a 10-year period. BA10 strains belonging to lineage 3 had large genetic distances (*p*-distance > 0.07). Thus, it may be possible to classify these strains as a new genotype, BA11. No positive selection site was detected in either genotype. Phylodynamic analyses showed that the effective population size of BA10 decreased gradually since 2010 and BA9 slightly decreased since 2009. The results suggested that the recently prevalent HRSV-B genotypes BA9 and BA10 evolved uniquely, leading to epidemics of HRSV-B worldwide over a 15-year period.

1. Introduction

Human respiratory syncytial virus (HRSV) belongs to the genus *Pneumovirus* in the family *Paramyxoviridae* and is a major causative virus for acute respiratory infection (ARI) (Leung et al., 2005). In particular, HRSV causes severe ARI, such as bronchitis, bronchiolitis, and pneumonia, in infants (Leung et al., 2005; Shay et al., 1999; Yorita et al., 2007). A previous report suggested that HRSV is associated with over 30% of pneumonia cases in infants (Hamano-Hasegawa et al., 2008). In addition, HRSV causes severe ARI, including pneumonia, in elderly people (Branche and Falsey, 2015; Lee et al., 2013). Thus, HRSV infection is a major disease burden causing respiratory infections in humans (Lee et al., 2013).

The HRSV genome encodes 10 genes and 11 proteins (Collins and Crowe, 2006), including two major antigens, the fusion (F) protein and attachment glycoprotein (G) (Collins and Crowe, 2006). The F protein is relatively highly conserved, while the G protein has a hypervariable region (Melero et al., 1997). This region also has epitopes for a neutralizing antibody against the G protein (Palomo et al., 1991). Mutations in the hypervariable region may lead to recurrent HRSV infections (Hall et al., 1991; Melero et al., 1997; Palomo et al., 1991).

HRSV is genetically classified into two subgroups, A (HRSV-A) and B (HRSV-B). These subgroups are further classified into many genotypes (Auksornkitti et al., 2014; Cui et al., 2013). Recent studies have suggested that HRSV-A and HRSV-B strains cluster into 12 genotypes (GA1–7, SAA1, NA1–2, and ON1–2) and 20 genotypes (GB1–4, BA1–10, SAB1–4, and URU1–2), respectively. Interestingly, HRSV-A genotypes ON1 and 2, and HRSV-B genotypes BA1–10 show unique tandem repeat insertions in the *G* gene, and these have emerged between the 1990s and 2010s (Auksornkitti et al., 2014; Hirano et al., 2014). The genotypes NA1, ON1, BA9, and

BA10 are the most prevalent types worldwide (Esposito et al., 2015; Kim et al., 2014).

Notably, the HRSV *G* gene evolves rapidly in HRSV-A, which is similar to the *HA* gene of influenza A virus (Hirano et al., 2014; Zhu et al., 2015). The C-terminal 3rd hypervariable regions of the *G* gene evolve rapidly in these strains, and include amino acid substitutions. Sites demonstrating negative and positive selection have been found in these regions (Hirano et al., 2014; Kushibuchi et al., 2013). However, the molecular evolution of the hypervariable region in the *G* gene of the prevalent HRSV-B genotypes BA9 and BA10 is not clear. Therefore, we studied the molecular evolution of the hypervariable region of the *G* gene in globally distributed HRSV-B strains belonging to genotypes BA9 and BA10.

2. Materials and Methods

2.1. Clinical Samples

Nasopharyngeal swabs were collected from 26 patients (age 20.6 months ± 13.6, mean ± standard deviation, SD) with acute respiratory infections, including upper respiratory infections (n = 4) and bronchitis (n = 22). Oral informed consent was obtained from all patients and/or their guardians. All samples were obtained between January 2009 and December 2014 in Fukui Prefecture. The study protocols were approved by the Ethics Committee of the National Institute of Infectious Diseases (approval no. 417). This study was carried out in accordance with the protocol.

2.2. RNA extraction, reverse transcription polymerase chain reaction, and sequencing

RNA extraction from the samples was performed using the QIAamp Viral RNA Mini Kit (Qiagen, Valencia, CA, USA). cDNA was synthesized using the PrimeScript RT Reagent Kit (Takara Bio, Otsu, Japan). PCR was performed using Takara Ex Taq (Takara Bio) under the following conditions: 95°C for 5 minutes, 30 cycles at 94°C for 1 minutes, 50°C for 1 minute, and 72°C for 2 minutes, followed by a final extension at 72°C for 7 minutes (Hirano et al., 2014; Peret et al., 1998). The primers used in this study were as follows; first PCR primer set, forward primer F1 (5′-CAACTCCATTGTTATTTGGC-3′), reverse primer GPB (5′-AAGATGATTACCATTTTGAAG-3′); second PCR primer set, forward primer F1, reverse primer GSB (5′-AAAACCAACCATCAAACCCAC-3′). Then, amplicons were purified with the MinElute PCR Purification Kit (Qiagen), and cycle sequenced using the BigDye Terminator v3.1 Cycle Sequencing Kit (Applied Biosystems, Foster City, CA, USA). The products were purified with the BigDyeX Terminator Purification Kit (Applied Biosystems) and analyzed with an ABI PRISM 3130 Genetic Analyzer

(Applied Biosystems). A Blast search was used to determine the RSV-B genotypes and to omit strains with 100% nucleotide sequence identity. Finally, 21 strains of genotype BA9 and 5 strains of genotype BA10 were detected from clinical samples and used in subsequent analyses.

2.3. Other strains used in this study

To comprehensively analyze the molecular evolution of genotypes BA9 and BA10, nucleotide sequences of the C-terminal 3rd hypervariable region of *G* sequences were obtained from GenBank. Other strains with representative genotypes belonging to RSV-B were collected. After the alignment of all strains using MEGA 6.0 (Tamura et al., 2013), those with 100% nucleotide sequence identity were omitted. A total of 77 strains belonging to genotype BA9, 61 strains of genotype BA10, and 34 strains of other HRSV-B genotypes were used. All strains included in the present study are shown in Table 1.

2.4. Phylogenetic analysis using the Bayesian Markov chain Monte Carlo method

To analyze the time-scaled phylogeny and evolutionary rate of the *G* gene, the Bayesian Markov chain Monte Carlo (MCMC) method was used as previously described (Hirano et al., 2014; Kushibuchi et al., 2013). The best nucleotide substitution model, the GTR-Γ model, was selected by KAKUSAN4 (Tanabe, 2011). Next, clock and demographic models were assessed by Bayes factor calculations (Kimura et al., 2015; Shiino et al., 2014; Suchard et al., 2001). For model selection, the ratio of two marginal likelihoods (AICM; Akaike's information criterion using MCMC) was estimated using Tracer v1.6 (http://tree.bio.ed.ac.uk/software/tracer/, Accessed: February 18, 2014). In the present study, four clock models were tested: a strict clock

model, an uncorrelated lognormal relaxed clock model, an uncorrelated exponential relaxed clock model, and a random local clock model. Simultaneously, four demographic models were tested: a constant size model, exponential growth model, logistic growth model, and expansion growth model. The AICM values for the clock and demographic models are shown in Table 2. Based on the data, MCMC trees were constructed using BEAST v1.7.5 (Drummond and Rambaut, 2007; Kimura et al., 2015). In the present study, the MCMC chains for all strains, genotype BA9, and genotype BA10 were run for 120,000,000 steps, 80,000,000 steps, and 200,000,000 steps and sampled every 4,000 steps, 2,000 steps, and 5,000 steps, respectively. Convergence was confirmed using Tracer v1.6 and effective sample size values above 200 after a 10% burn-in were accepted (Hirano et al., 2014; Kimura et al., 2015). The maximum clade credibility tree was generated by Tree Annotator v 1.7.4 after removing the first 10% of trees as a burn-in. Finally, the phylogenetic tree was viewed in FigTree v1.4.0 (http://tree.bio.ed.ac.uk/software/figtree/, Accessed: August 3, 2013). The evolution rates were also calculated using BEAST v1.7.5 under the above models (Drummond and Rambaut, 2007).

2.5. Phylogenetic trees constructed by the maximum likelihood method

To estimate the genetic distances and characterize the lineages, phylogenetic trees were also constructed using the maximum likelihood (ML) method with the GTR-Γ model implemented in PhyML3.0. (Guindon et al., 2010). The best substitution model was determined using KAKUSAN4. The reliability of the tree was estimated using 1,000 bootstrap replications.

2.6. Estimation of pairwise distances (p-distances) among strains

To assess the frequency distribution of the RSV-B strains, including genotypes BA9 and BA10, the *p*-distances were calculated using MEGA 6.0 as previously described (Hirano et al., 2014; Tamura et al., 2013).

2.7. Selective pressure analysis

To analyze the selective pressure on the *G* gene, synonymous (*dS*) and nonsynonymous (*dN*) substitutions at every codon were calculated by Datamonkey using the single likelihood ancestor (SLAC) method, fixed effects likelihood (FEL) method, and internal fixed effects likelihood (IFEL) method (Hirano et al., 2014; Pond and Frost, 2005a; Pond and Frost, 2005b). The cut-off *p*-value was set at 0.05.

2.8. Bayesian skyline plot (BSP) analysis

Changes in the effective population size of genotypes BA9 and BA10 were analyzed using a Bayesian skyline plot analysis implemented BEAST v1.7.4 as previously described (Drummond and Rambaut, 2007; Drummond et al., 2005). The best substitution model was GTR-Γ according to KAKUSAN4. The clock model data are shown in Table 3. The MCMC chains of all BA genotypes, genotype BA9 alone, and genotype BA10 alone were run for 300,000,000 steps, 150,000,000 steps, and 100,000,000 steps and sampled every 6,000 steps, 3,000 steps, and 5,000 steps, respectively.

2.9. Statistical analysis

Statistical analyses were performed using Mann-Whitney U method by PASW Statistics 18. Values of $p < 0.05$ were considered to be significant.

3. Results

3.1. Phylogeny of HRV-B genotypes BA based on the MCMC method

To estimate the time-scale evolution of the C-terminal 3rd hypervariable region of the *G* gene in all HRV-B genotypes, including BA9 and BA10, we constructed phylogenetic trees using the MCMC method (Figure 1). The first BA genotype that arose, BA1, had a tandem repeat insertion (60 nt) and diverged from genotype GB3. Genotype BA10 diverged from the ancestors of genotypes BA7 and BA8. In addition, genotype BA9 diverged from the ancestors of genotypes BA7, BA8, and BA10. We estimated that genotype BA1 and GB3 diverged in 1997 (95% highest posterior density, HPD; 1994–1999). BA9 and BA10 diverged in 1999 (95% HPD; 1994–2003) and 2001 (HPD95%; 1997–2004), respectively (Table 4). Furthermore, the recently prevalent genotypes BA9 and BA10 formed three lineages. Detailed information regarding the divergence times of each lineage is shown in Figure 1.

Next, we assessed the evolutionary rates of the present strains using the MCMC method (Table 4). We did not detect significant differences in divergence rates between HRSV-B and genotypes BA9 and BA10. The results suggested that these genotypes emerged and evolved rapidly and independently for 15 years.

3.2. Phylogeny of HRSV-B genotypes BA9 and BA10 based on the maximum likelihood method

To determine genetic distances and common areas for the recent prevalent HRSV-B genotypes BA9 and BA10, we also constructed phylogenetic trees using the ML method (Figure 2). The BA9 strains belonging to lineages 1 and 3 were detected in various regions (including in Africa, Asia, Europe, North America, and South America), while lineage 2 was detected exclusively in Asian areas. The BA10 strains belonging to

lineages 2 and 3 were detected in Asian areas, while those belonging to lineage 1 were distributed more broadly, similar to strains belonging to the BA9 genotype. These results suggested that genotypes BA9 and BA10 are widespread, but some lineages could have relatively limited distributions, although the present data may have a selection bias.

3.3. The pairwise distances (p-distances) of the BA9 and BA10 strains

To assess the genetic distances among the strains belonging to all BA genotypes, genotype BA9, and genotype BA10, we calculated *p*-distances. As shown in Figure 3, the *p*-distances of strains for all BA genotypes were 0.039 ± 0.016 (mean ± standard deviation, SD). In addition, the *p*-distances of the strains belonging to genotypes BA9 and BA10 were 0.023 ± 0.010 and 0.044 ± 0.018, respectively. The *p*-distances of BA10 were significantly larger than those of BA9 ($p < 0.05$). The *p*-distances among all BA9 strains were < 0.07. Notably, the *p*-distances of the strains belonging to genotype BA10 lineage 3 were 0.074 to 0.091, when compared with a BA10 strain (GenBank accession no. AB776000) belonging to lineage 1. This suggested genetic divergence within the BA10 strains was larger than within BA9 strains. Previous reports have suggested that the *p*-distances for strains with the same genotype are < 0.07 (Venter et al., 2001). Thus, the strains belonging to BA10 lineage 3 could be classified as candidates of a new genotype, BA11.

3.4. Positive and negative selection sites in HRSV-B genotype BA

We identified sites exhibiting positive and negative selection in the region using SLAC, FEL, and IFEL (Table 5 and 6). Previous reports have suggested that a suitable estimate of sites that show evidence for positive selection may be accepted by all three

methods (Botosso et al., 2009; Kimura et al., 2015). We found two sites showing evidence of positive selection in the analysis of all BA genotypes (Y287H and H287Y). However, no sites exhibited positive selection in genotypes BA9 and BA10 in the analyzed regions. We detected eight sites under negative selection in the analysis of all genotypes (A220, L252, H279, Q282, P291, L291, Q299, and S304). In genotype BA9 strains, we detected two negative selection sites (P295 and S304), and we detected three negative selection sites (L272, P291, and S304) in BA10. These results suggested that strains with genotypes BA9 and BA10 did not experience strong selective pressure in the host.

3.5. Bayesian skyline plot (BSP) analysis

We estimated effective population sizes used a coalescent-based BSP analysis. As shown in Figure 4, the effective population sizes for all BA genotypes gradually increased from 2002–2005, and then decreased in 2006, after which a constant size was maintained. However, the population size of genotype BA9 remained constant from 2003 to 2009, and then slightly decreased. In addition, the population size of genotype BA10 was constant from 2004 to 2010, and then decreased gradually thereafter. These results suggested that the effective population size dynamics were genotype-specific.

4. Discussion

We analyzed the molecular evolution of the C-terminal 3rd hypervariable regions of the *G* gene in HRSV-B genotypes BA9 and BA10 (which are currently prevalent). We found that the BA9 genotype diverged from the common ancestor of the BA7, BA8, and BA10 genotypes, while the BA10 genotype diverged from the common ancestor of the BA7 and BA8 genotypes (Figure 1). We estimated that BA9 and BA10 diverged between 1999 and 2001. Strains of both genotypes (BA9 and BA10) evolved rapidly (approximately 4.8×10^{-3} substitutions/site/year) and formed three lineages within about 10 years. We could not find the positive selection site in either BA9 or BA10. Furthermore, BA10 strains belonging to lineage 3 had large genetic distances (*p*-distances > 0.07). The effective population size of all BA genotypes was constant, while BA10 gradually decreased since 2010. These results indicated that the genotypes arose and evolved rapidly and independently, causing epidemics of HRSV-B infections in various areas.

HRSV-B genotype BA1 was initially detected in 1999 in Buenos Aires, Argentina (Trento et al., 2003). This genotype has a unique tandem repeat insertion in the C-terminal hypervariable region of the *G* gene and spread rapidly, including in Europe, the United States, Japan, and Africa (Bose et al., 2015; Dapat et al., 2010; Esposito et al., 2015; Pretorius et al., 2013). Furthermore, our time-scale evolutionary trees estimated using MCMC methods showed that the BA1 strains have diverged substantially, leading to the emergence of many new genotypes (BA2 to BA10) since 1997. BA9 and BA10 are recently prevalent genotypes (Esposito et al., 2015). However, the precise processes by which these genotypes have evolved are unknown. Therefore, we analyzed the molecular evolution of these genotypes using global samples. Both genotypes, BA9 and BA10, emerged between 1999 and 2001. This estimate is not compatible with the years

in which BA1 has been detected (Trento et al., 2003). This incompatible time estimate has been reported for another subgroup/genotype of HRSV-A/ON1, which has a tandem repeat insertion in the *G* gene as well the BA genotypes of HRSV-B (Hirano et al., 2014), but the reasons for these observations are unclear at present.

Previous reports have suggested that the C-terminal hypervariable region evolved rapidly, similar to the *HA* gene in influenza A virus. For example, Kushibuchi et al. estimated the evolutionary rates of the C-terminal 3rd hypervariable region in both HRSV-A and HRSV-B strains (Kushibuchi et al., 2013). They showed that HRSV-B strains evolved more quickly than HRSV-A strains (HRSV-A, 3.63×10^{-3} substitutions/site/year; HRSV-B, 4.56×10^{-3} substitutions/site/year). In addition, Hirano et al. examined the same region in HRSV-A and found that ON1 evolved at a faster rate than the ancestral genotype NA1 (ON1, 6.03×10^{-3} substitutions/site/year; NA1, 4.61×10^{-3} substitutions/site/year) (Hirano et al., 2014). We estimated the evolutionary rates of the BA genotypes of HRSV-B. The observed rates of evolution for HRSV-B are similar to those previously reported for HRSV-A. Thus, the *G* gene of HRSV-B BA genotypes may evolve rapidly, in a similar manner to other HRSV strains such as HRSV-A (Hirano et al., 2014).

Furthermore, we assessed the genetic distances among the BA9 and BA10 strains (Figure 3). It has been suggested that within a genotype, the *p*-distances are < 0.07 (Venter et al., 2001). Notably, the *p*-distances among some strains of BA10 exceeded 0.07. These strains belonged to lineage 3 and were detected in Asian regions (India, Japan, Malaysia, Thailand, and Vietnam). These strains diverged around 2008 (Figure 1). Accordingly, these strains could be classified into a new genotype, BA11. In contrast, the *p*-distance values among all BA9 strains were < 0.07. Moreover, a very recent study proposed for a new classification of HRSV-A using *p*-distance calculation

method (Trento et al., 2015). Based on this method, it is possible that an alteration of the classification of HRSV-B genotypes may be required, including a new candidate genotype, namely BA11 (Trento et al., 2015).

It has been suggested that the evolution of viral antigens are associated with recurrent infections in the host, leading to viral reinfections (Domingo, 2006). For example, the rapid evolution of the *HA* gene in seasonal influenza viruses, such as a subtype A (H3N2), is strongly associated with the ability of influenza to reinfect (Taubenberger and Kash, 2010). Similarly, the evolution of the HRSV *G* gene, which exhibits positive selection, might be linked to HRSV reinfection (Botosso et al., 2009; Collins and Melero, 2011). Thus, we identified positive selection at sites in the *G* gene of genotype BA strains (Table 5). Consider all genotype BA strains, positive selection sites (H287Y and Y287H) were estimated using three methods (SLAC, FEL, and IFEL). However, no positive selection site was detected in the strains of either genotype BA9 or BA10 using all three methods (Table 5). In addition, our previous report suggested a lack of positive selection using the same three methods in another prevalent HRSV-A genotype, ON1 (Hirano et al., 2014). These results suggested that the BA genotypes are not significantly affected by selective pressures in the host (Domingo, 2006).

We also estimated negative selection for sites in the present strains. In general, negative selection plays a role in preventing the functional deterioration of various viruses (Domingo, 2006). For example, Domingo et al. demonstrated that negative selection in neutralization epitopes of polioviruses was involved in receptor recognition and in the formation of altered virions (Domingo et al., 1993). The roles of negative selection at sites in the HRSV G protein are not clear; however, it is possible that these amino acid substitutions act in the prevention of antigenic deterioration (Domingo, 2006; Hirano et al., 2014).

Moreover, we assessed the phylodynamics of the *G* gene based on effective population size estimates using BSP analyses. For all BA genotypes, the effective population size was relatively constant over the past 15 years. However, the sizes of BA9 and BA10 gradually decreased for the past 5 years (Figure 4). The prevalence of BA9 and BA10 strains may gradually decline in the near future based on our analysis of the partial sequence of the G gene.

5. Conclusion

The C-terminal hypervariable region of the *G* gene in HRSV-B strains with BA genotypes, including BA9 and BA10, emerged approximately 15 years ago and evolved rapidly. Furthermore, some BA10 strains may represent a new genotype, BA11, based on their divergence levels. Phylodynamic analyses of BA10 suggest that its prevalence may decline in the near future. However, further surveillance is needed to confirm this inference.

Acknowledgements

I thank Dr. Akihide Ryo, Dr. Kazunori Oishi, Dr. Masatsugu Obuchi, Dr. Naruhiko Ishiwada, Dr. Masahiro Noda and Dr. Kuroda. Ms. Miho Kobayashi instruct me in molecular systematic analysis. I also thank Dr. Eiko Hirano who collected clinical samples. I feel deep appreciating for Dr. Hirokazu Kimura and Dr. Naoki Shimojo who supervised this study. The work was partially supported by Grant-in-Aid from the Japan Society for the Promotion of Science and for Research on Emerging and Re-emerging Infectious Diseases from the Japanese Ministry of Health, Labour and Welfare (H25-Shinko-Ippan-010) and the Japan Agency for Medical Research and Development.

Competing interests

The authors declare that they have no competing interests.

References

Auksornkitti, V., Nichaphat, K., Siwanat, T., Kamol, S., Apiradee, T., Rujipat, S., Yong, P., 2014. Molecular characterization of human respiratory syncytial virus, 2010-2011: identification of genotype ON1 and a new subgroup B genotype in Thailand. Arc. Virol. 159, 499-507.

Bose, M.E., Jie, H., Susmita, S., NelsonI, M.I., Jayati, B., Halpin R.A., Town, C. D., Lorenzi H. A., Noyola D.E., Falcone, V., Gerna, G., Bnhouwer H.D., Videla, C.V., Kok, T., Venter, M., Henrickson, K.J., 2015. Sequencing and analysis of globally obtained human respiratory syncytial virus A and B genomes. PloS One 10, e0120098.

Botosso, V.F., Zanotto,.P.M., Ueda, M., Arruda, E., Gilio, A.E., Vieria, S.E., Stewien, K.E., Peret, T.E., Jamal, L.F., Pardini, M.I., Pinho J.R., Massad, E., Sant'Anna, O.A., Holmes, E.C., Durigon, E.L., the VGDN Consortium, 2009. Positive selection results in frequent reversible amino acid replacements in the *G* protein gene of human respiratory syncytial virus. PLoS pathog. 5, e1000254.

Branche, A.R., Falsey, A.R., 2015. Respiratory syncytial virus infection in older adults: an under-recognized problem. Drugs & aging 32, 261-269.

Collins, P.L., Crowe, Jr., J.E., 2006. Respiratory syncytial virus and metapneumovirus. In: Knipe, D.M., Howley, P.M., Griffin, D.E., Martin, M.A., Lamb, R.A., Roizman, B., Straus, S.E. (Eds.), Fields Virology, fifth ed. Lippincott Williams & Wilkins, Philadelphia, pp.1601-1646.

Collins, P.L., Melero, J.A., 2011. Progress in understanding and controlling respiratory syncytial virus: still crazy after all these years. Virus Res. 162, 80-99.

Cui, G., Zhu, R., Qian, Y., Deng, J., Zhao, L., Sun, Y., Wang, F., 2013. Genetic variation in

attachment glycoprotein genes of human respiratory syncytial virus subgroups A and B in children in recent five consecutive years. PLoS One. 8, e75020.

Dapat, I.C., Shobugawa, Y., Sano, Y., Saito, R., Sasaki, A., Suzuki, Y., Kumaki, A., Zaraket, H., Dapat, C., Oguma, T., Yamaguchi, M., Suzuki, H., 2010. New genotypes within respiratory syncytial virus group B genotype BA in Niigata, Japan. J. Clin. Microbiol. 48, 3423-3427.

Domingo, E., Diez, J., Martinez, M.A., Hernandez, J., Holguin, A., Borrego, B., Mateu, M., 1993. New observations on antigenic diversification of RNA viruses. Antigenic variation is not dependent on immune selection. J. Gen. Virol. 74, 2039-2045.

Domingo, E., 2006. Virus evolution, in: Knipe, D.M., Howley, P.M., Griffin, D.E., Martin, M.A., Lamb, R.A., Roizman, B., Straus, S.E. (Eds.), Fields Virology, fifth ed. Lippincott Willams&Wilkins, Philadelphia, pp. 389–421.

Drummond, A.J., Rambaut, A., Shapiro, B., Pybus, O.G., 2005. Bayesian coalescent inference of past population dynamics from molecular sequences. Mol. Biol. Evol. 22, 1185-1192.

Drummond, A.J., Rambaut, A., 2007. BEAST: Bayesian evolutionary analysis by sampling trees. BMC Evol. Biol. 7, 214.

Esposito, S., Piralla, A., Zampiero, A., Bianchini, S., Pietro, G.D. Scala, A., Pinzani, R., Fossali, E., Baldanti, F., Principi, N., 2015. Characteristics and Their Clinical Relevance of Respiratory Syncytial Virus Types and Genotypes Circulating in Northern Italy in Five Consecutive Winter Seasons. PloS One 10, e0129369.

Guindon, S., Jean-Francois, D., Lefort, V., Anisimova, M., Hordijk, W., Gascuel, O., 2010. New algorithms and methods to estimate maximum-likelihood phylogenies: assessing the performance of PhyML 3.0. Systematic Biol. 59, 307-321.

Hall, C.B., Walsh, E.E., Long, C.E., Schnabel, K.C., 1991. Immunity to and frequency of reinfection with respiratory syncytial virus. J. Infect. Dis. 163, 693–698.

Hamano-Hasegawa, K., Morozumi, M., Nakayama, E., Chiba, N., Murayama, S.Y., Takayanagi,

R., Iwata, S., Sunakawa, K., Ubukata, K., 2008. Comprehensive detection of causative pathogens using real-time PCR to diagnose pediatric community-acquired pneumonia. J. Infect. Chemother. 14, 424-432.

Hirano, E., Kobayashi, M., Tsukagoshi, H., Yoshida, L.M., Kuroda, M., Noda, M., Ishioka, T., Kozawa, K., Ishii, H., Yoshida, A., Oishi, K., Ryo, A., Kimura, H., 2014. Molecular evolution of human respiratory syncytial virus attachment glycoprotein (*G*) gene of new genotype ON1 and ancestor NA1. Infect. Geneti and Evol. 28, 183-191.

Kim, Y.J., Kim, D.W., Lee, W.J., Yun, M.R., Lee, H.Y., Lee, H.S., Jung, H.D., Kim, K., 2014. Rapid replacement of human respiratory syncytial virus A with the ON1 genotype having 72 nucleotide duplication in *G* gene. Infect. Genet. Evol. 26C, 103–112.

Kimura, H., Saitoh, M., Kobayashi, M., Ishii, H., Saraya, T., Kurai, D., Tsukagoshi, H., Shirabe, K., Nishina, A., Kozawa, K., Kuroda, M., Takeuchi, F., Sekizuka, T., Minakami, H., Ryo, A., Takeda, M., 2015. Molecular evolution of haemagglutinin (*H*) gene in measles virus. Sci. Rep. 5, 11648.

Kushibuchi, I., Kobayashi, M., Kusaka, T., Tsukagoshi, H., Ryo, A., Yoshida, A., Ishii, H., Saraya, T., Kurai, D., Yamamoto, N., Kanou, K., Saitoh, M., Noda, M., Kuroda, M., Morita, Y., Kozawa, K., Oishi, K., Tashiro, M., Kimura, H., 2013. Molecular evolution of attachment glycoprotein (*G*) gene in human respiratory syncytial virus detected in Japan 2008-2011. Infect. Genet. Evol. 18, 168–173.

Lee, N., Lui, G.C., Wong, K.T., Li, T.C., Tse, E.C., Chan, J.Y., Yu, J., Wong, S.S., Choi, K.W., Wong, R.Y., Ngai, K.L., Hui, D.S., Chan, P.K., 2013. High morbidity and mortality in adults hospitalized for respiratory syncytial virus infections. Clin. Infect. Dis. 57, 1069–1077.

Leung, A.K., Kellner, J.D., Davies, H.D., 2005. Respiratory syncytial virus bronchiolitis. J. Natl. Med. Assoc. 97, 1708–1713.

Melero, J.A., García-Barreno, B., Martínez, I., Pringle, C.R., Cane, P.A., 1997. Antigenic structure, evolution and immunobiology of human respiratory syncytial virus attachment (G) protein. J. Gen. Virol. 78, 2411–2418.

Palomo, C., García-Barreno, B., Peñas, C., Melero, J.A., 1991. The G protein of human respiratory syncytial virus: significance of carbohydrate side-chains and the C-terminal end to its antigenicity. J. Gen. Virol. 72, 669–675.

Peret, T.C., Hall, C.B., Schnabel, K.C., Golub, J.A., Anderson, L.J., 1998. Circulation patterns of genetically distinct group A and B strains of human respiratory syncytial virus in a community. J. Gen. Virol. 79, 2221–2229.

Pond, S.L., Frost, S.D., 2005a. Datamonkey: rapid detection of selective pressure on individual sites of codon alignments. Bioinformatics. 21, 2531–2533.

Pond, S.L., Frost, S.D., 2005b. Not So Different After All: A Comparison of Methods for Detecting Amino Acid Sites Under Selection. Mol. Biol. Evol. 22,1208-1222.

Pretorius, M. A., van Niekerk, S., Tempia, S., Moyes, J., Cohen, C., Madhi, S.A., Venter, M., SARI Surveillance Group, 2013. Replacement and positive evolution of subtype A and B respiratory syncytial virus G-protein genotypes from 1997-2012 in South Africa. J. Infect. 208, S227–237.

Shay, D.K., Holman, R.C., Newman, R.D., Liu, L.L., Stout, J.W., Anderson, L.J., 1999. Bronchiolitis-associated hospitalizations among US children, 1980–1996. JAMA. 282, 1440–1446.

Shiino, T., Hattori, J., Yokomaku, Y., Iwatani, Y., Sugiura, W., 2014. Phylodynamic Analysis Reveals CRF01_AE Dissemination between Japan and Neighboring Asian Countries and the Role of Intravenous Drug Use in Transmission. PLoS One 9, e10263.

Suchard, M.A., Weiss, R.E., Sinsheimer, J.S. 2001. Bayesian selection of continuous-time Markov chain evolutionary models. Mol. Biol. Evol. 18, 1001-1013.

Tamura, K., Stecher, G., Peterson, D., Filipski, A., Kumar, S., 2013. MEGA6: Molecular Evolutionary Genetics Analysis version 6.0. Mol. Biol. Evol. 30, 2725–2729.

Tanabe, A.S., 2011. Kakusan4 and Aminosan: two programs for comparing nonpartitioned, proportional and separate models for combined molecular phylogenetic analyses of multilocus sequence data. Mol. Ecol. Resour. 11, 914–921.

Taubenberger, J.K., Kash, J.C., 2010. Influenza virus evolution, host adaptation, and pandemic formation. Cell Host Microbe. 7, 440–451.

Trento, A., Ábrego, L., Rodriguez-Fernandez, R., González-Sánchez, M.I., González-Martínez, F., Delfraro, A., Pascale, J.M., Arbiza, J., Melero, J.A., 2015. Conservation of G-Protein Epitopes in Respiratory Syncytial Virus (Group A) despite Broad Genetic Diversity: Is Antibody Selection Involved in Virus Evolution? J. Virol. 89, 7776-7785.

Trento, A., Galiano, M., Videla, C., Carballal, G., García-Barreno, B., Melero, J.A., Palomo, C., 2003. Major changes in the G protein of human respiratory syncytial virus isolates introduced by a duplication of 60 nucleotides. J. Gen. Virol. 84, 3115–3120.

Venter, M., Madhi, S.A., Tiemessen, C.T., Schoub, B.D., 2001. Genetic diversity and molecular epidemiology of respiratory syncytial virus over four consecutive seasons in South Africa: identification of new subgroup A and B genotypes. J. Gen. Virol. 82, 2117–2124.

Yorita, K.L., Holman, R.C., Steiner, C.A., Effler, P.V., Miyamura, J., Forbes, S., Anderson, L.J., Balaraman, V., 2007. Severe bronchiolitis and respiratory syncytial virus among young children in Hawaii. Pediatr. Infect. Dis. J. 26, 1081–1088.

Zhu, H., Hughes, J., Murcia, P.R., 2015. Origins and Evolutionary Dynamics of H3N2 Canine Influenza Virus. J. Virol. 89, 5406–5418.

Table.1. HRSV-B strains used in this study

Strain	GenBank accession No.	Collection year	Country	Genotype
RSV/YOK/07/56	AB551093	2007	Japan	BA10
Gunma/775/2010	AB683226	2010	Japan	BA10
Tochigi/336/2008	AB775985	2008	Japan	BA10
Tochigi/57/2010	AB775987	2010	Japan	BA10
Tochigi/60/2010	AB775989	2010	Japan	BA10
Tochigi/157/2011	AB776000	2011	Japan	BA10
RSvi/Okinawa.JPN/5.11	AB900747	2011	Japan	BA10
1936/BKK/07	FJ490355	2008	Thailand	BA10
2580/BKK/07	FJ490360	2008	Thailand	BA10
MAD/5662/06-07	GQ150729	2007	Spain	BA10
MAD/5745/06-07	GQ150734	2007	Spain	BA10
NG-042-07	HM459884	2007	Japan	BA10
NG-077-07	HM459886	2007	Japan	BA10
NG-017-07	HM459890	2007	Japan	BA10
NG-065-07	HM459891	2007	Japan	BA10
NG-050-09	HM459892	2009	Japan	BA10
SA1507096OP	HQ711816	2008	South Africa	BA10
Cam2007-6084	JN119960	2007	Cambodia	BA10
Cam2008-3125	JN119964	2008	Cambodia	BA10
Cam2008-3393	JN119966	2008	Cambodia	BA10
Cam2008-9297	JN119972	2008	Cambodia	BA10
Cam2009-1240	JN119982	2009	Cambodia	BA10
Cam2009-2120	JN119984	2009	Cambodia	BA10
Cam2009-5023	JN119991	2009	Cambodia	BA10
Cam2009-5091	JN119994	2009	Cambodia	BA10
Cam2009-5148	JN119995	2009	Cambodia	BA10
Cam2009-8186	JN120009	2009	Cambodia	BA10
Cam2009-9165	JN120014	2009	Cambodia	BA10
BR_CE_228_2008	JQ806037	2008	Brazil	BA10
HR18939-08	JQ844874	2008	Croatia	BA10
UPM/B/03	JQ933953	2009	Malaysia	BA10
UPM/B/09	JQ933959	2009	Malaysia	BA10
UPM/B/11	JQ933961	2009	Malaysia	BA10
UPM/B/12	JQ933962	2009	Malaysia	BA10
UPM/B/18	JQ933968	2009	Malaysia	BA10
566-HCM/07.10-BA10	JX079990	2010	Viet Nam	BA10
800-HCM/09.10-BA10	JX079991	2010	Viet Nam	BA10
960-HCM/11.10-BA10	JX079993	2010	Viet Nam	BA10
MY-2246492-09	JX256973	2009	Malaysia	BA10
MY-2134333-09	JX256974	2009	Malaysia	BA10
MY-2238278-09	JX256979	2009	Malaysia	BA10
MY-1819620-07	JX256981	2007	Malaysia	BA10
BE/5923/06	JX645880	2006	Belgium	BA10

Strain	GenBank accession No.	Collection year	Country	Genotype
BE/9364/09	JX645881	2009	Belgium	BA10
BE/5489/08	JX645885	2008	Belgium	BA10
BJ/20240	KC297426	2009	China	BA10
BJ/20624	KC297433	2009	China	BA10
BJ/F6832	KC297481	2008	China	BA10
CU_C694	KC342327	2010	Thailand	BA10
CU_C1101	KC342329	2010	Thailand	BA10
CU_C1182	KC342332	2010	Thailand	BA10
SA01-00170	KC476929	2009	South Africa	BA10
SA01-00475	KC476950	2009	South Africa	BA10
SA01-01138	KC476965	2009	South Africa	BA10
SA01-06825	KC476988	2009	South Africa	BA10
SA02-00482	KC476995	2010	South Africa	BA10
SA2644	KC477093	2012	South Africa	BA10
LV/041/11	KF030165	2011	Latvia	BA10
RSV/PUNE/NIV0934544/09/B	KF246585	2009	India	BA10
RSV/PUNE/NIV0931702/09/B	KF246586	2009	India	BA10
HD22098	KJ710408	2013	Germany	BA10
Fukui/002/2012	LC060579	2012	Japan	BA10
Fukui/059/2014	LC060580	2014	Japan	BA10
Fukui/142/2011	LC060581	2011	Japan	BA10
Fukui/178/2009	LC060582	2009	Japan	BA10
Fukui/238/2013	LC060583	2013	Japan	BA10
RSV/YOK/07/67	AB551099	2007	Japan	BA9
NG-102-06	AB603467	2006	Japan	BA9
NG-108-05	AB603470	2005	Japan	BA9
Gunma/470/2009	AB683224	2009	Japan	BA9
Gunma/777/2010	AB683227	2010	Japan	BA9
Gunma/778/2010	AB683228	2010	Japan	BA9
Gunma/807/2010	AB683230	2010	Japan	BA9
Kumamoto/9941/2010	AB683237	2010	Japan	BA9
Tochigi/81/2010	AB775991	2010	Japan	BA9
Tochigi/149/2010	AB775993	2010	Japan	BA9
Tochigi/375/2010	AB775997	2010	Japan	BA9
Tochigi/511/2011	AB775999	2011	Japan	BA9
49RSVB	AB831568	2012	Japan	BA9
RSvi/Okinawa.JPN/310.11	AB900759	2011	Japan	BA9
RSV/Ibaraki/01/2014	AB918645	2014	Japan	BA9
BA/100/2004	DQ227395	2004	Argentina	BA9
BR259-2005	EU582474	2005	Brazil	BA9
MAD/4540/04-05	GQ150707	2004	Spain	BA9
NG-040-07	HM459879	2007	Japan	BA9
493-HCM/06.10-BA9	JJX079975	2010	Viet Nam	BA9
812-HCM/09.10-BA9	JJX079980	2010	Viet Nam	BA9

Strain	GenBank accession No.	Collection year	Country	Genotype
Cam2008-7298	JN119970	2008	Cambodia	BA9
Cam2009-5090	JN119993	2009	Cambodia	BA9
BR_CE_170_2007	JQ806031	2007	Brazil	BA9
BR_CE_291_2007	JQ806044	2007	Brazil	BA9
BR_CE_316_2004	JQ806048	2004	Brazil	BA9
BR_CE_358_2006	JQ806050	2006	Brazil	BA9
HR2085-06	JQ844871	2006	Croatia	BA9
HR14602-06	JQ844873	2006	Croatia	BA9
UPM/B/21	JQ933971	2009	Malaysia	BA9
522-HCM/06.10-BA9	JX079976	2010	Viet Nam	BA9
861-HCM/10.10-BA9	JX079983	2010	Viet Nam	BA9
889-HCM/10.10-BA9	JX079985	2010	Viet Nam	BA9
TX-79307	JX198151	2005	USA	BA9
MY-1680661-06	JX256993	2006	Malaysia	BA9
HD/70190423/12	JX967575	2012	Germany	BA9
BJ/20678	KC297434	2009	China	BA9
BJ/35164	KC297475	2012	China	BA9
BJ/35435	KC297476	2012	China	BA9
BJ/F5610	KC297480	2007	China	BA9
CU_C423	KC342326	2009	Thailand	BA9
CU2010/18	KC342338	2010	Thailand	BA9
CU2011/59	KC342341	2011	Thailand	BA9
CU2011/99	KC342344	2011	Thailand	BA9
CU2011/205	KC342347	2011	Thailand	BA9
CQ2588-1211	KC461264	2011	China	BA9
SA01-00607	KC476954	2009	South Africa	BA9
SA03-00635	KC476998	2010	South Africa	BA9
SA01-06849	KC477012	2011	South Africa	BA9
SA01-07016	KC477014	2011	South Africa	BA9
SA01-07052	KC477020	2011	South Africa	BA9
SA01-07128	KC477026	2011	South Africa	BA9
SA01-07492	KC477035	2011	South Africa	BA9
SA01-07509	KC477036	2011	South Africa	BA9
SA05-01273	KC477076	2011	South Africa	BA9
SA05-01411	KC477077	2011	South Africa	BA9
SA05-04145	KC477078	2011	South Africa	BA9
SA2090	KC477084	2012	South Africa	BA9
RSV/PUNE/NIV0934728/09/B	KF246589	2009	India	BA9
RSV/PUNE/NIV0936145/09/B	KF246592	2009	India	BA9
SH10012507BA9	KJ658807	2010	China	BA9
DEL/S190P/10	KJ690598	2010	India	BA9
HD22271	KJ710412	2013	Germany	BA9
HD24154	KJ710414	2013	Germany	BA9
HD24250	KJ710417	2013	Germany	BA9

Strain	GenBank accession No.	Collection year	Country	Genotype
HD24278	KJ710419	2013	Germany	BA9
P92	KJ938292	2013	Germany	BA9
TBp-12-0073	KM873461	2012	Philippines	BA9
TBp-13-0012	KM873463	2013	Philippines	BA9
TBp-13-0045	KM873467	2013	Philippines	BA9
TBp-13-0079	KM873471	2013	Philippines	BA9
TBp-13-0130	KM873476	2013	Philippines	BA9
TBp-13-0179	KM873479	2013	Philippines	BA9
TEv-13-0259	KM873488	2013	Philippines	BA9
TOp-12-0185	KM873490	2012	Philippines	BA9
TOp-13-0128	KM873497	2013	Philippines	BA9
IND/HRSVB/LKO/13/0501	KP269185	2013	India	BA9
Fukui/026/2014	LC060564	2014	Japan	BA9
Fukui/027/2014	LC060565	2014	Japan	BA9
Fukui/048/2014	LC060566	2014	Japan	BA9
Fukui/073/2012	LC060567	2012	Japan	BA9
Fukui/093/2014	LC060568	2014	Japan	BA9
Fukui/105/2014	LC060569	2014	Japan	BA9
Fukui/120/2014	LC060570	2014	Japan	BA9
Fukui/130/2014	LC060571	2014	Japan	BA9
Fukui/143/2013	LC060572	2013	Japan	BA9
Fukui/144/2013	LC060573	2013	Japan	BA9
Fukui/144/2014	LC060574	2014	Japan	BA9
Fukui/148/2011	LC060575	2011	Japan	BA9
Fukui/162/2013	LC060576	2013	Japan	BA9
Fukui/197/2013	LC060577	2013	Japan	BA9
Fukui/211/2013	LC060578	2013	Japan	BA9
Fukui/221/2014	LC060584	2014	Japan	BA9
Fukui/243/2013	LC060585	2013	Japan	BA9
Fukui/305/2013	LC060586	2013	Japan	BA9
Fukui/421/2014	LC060587	2014	Japan	BA9
Fukui/506/2014	LC060588	2014	Japan	BA9
Fukui/520/2014	LC060589	2014	Japan	BA9
NG-228-06	HM459871	2006	Japan	BA8
NG-013-07	HM459873	2007	Japan	BA8
NG-068-05	HM459864	2005	Japan	BA7
NG-095-05	HM459865	2005	Japan	BA7
BE/11500/01	AY751105	2001	Belgium	BA6
NG-004-03	AB175819	2003	Japan	BA5
NG-109-05	AB603471	2005	Japan	BA4
BE/13689/04	DQ985150	2004	Belgium	BA3
NG-153-03	AB175821	2003	Japan	BA2
BA4128/99B	AY333364	1999	Argentina	BA1
Mon/15/90	AY333361	1990	Uruguay	URU2

Strain	GenBank accession No.	Collection year	Country	Genotype
Mon/6/01	AY488803	2001	Uruguay	URU2
Mon/7/01	AY488804	2001	Uruguay	URU1
Cam2009-8166	JN120007	2009	Cambodia	SAB4
SA98V192	AF348811	1998	South Africa	SAB3
SA99V429	AF348813	1999	South Africa	SAB3
Moz/205/99	AF309678	1999	Mozambique	SAB2
SA99V800	AF348821	1999	South Africa	SAB2
SA99V1325	AF348822	1999	South Africa	SAB2
SA0025	AF348825	2000	South Africa	SAB1
SA98D1656	AF348826	1998	South Africa	SAB1
Ken/109/02	AY524573	2002	Kenya	SAB1
SA98V602	AF348824	1998	South Africa	GB4
BA/3018/98	AY672691	1998	Argentina	GB4
BA/3976/99	AY672698	1999	Argentina	GB4
TX-65859	JX198144	1994	USA	GB3
CH93-9b	AF065251	1993	USA	GB2
NZB_88_01	DQ171849	1988	New Zealand	GB2
NZB_89_01	DQ171858	1989	New Zealand	GB2
CH10b	AF065250	1990	USA	GB1
WV4843	M73540	1980	USA	GB1
WV/10010	M73541	1983	USA	GB1
WV15291	M73542	1985	USA	GB1
CH/18537	M17213	1962	USA	

Table 2. Model comparison based on Akaike's information criterion for MCMC (AICM) for the phylogenetic analysis

a) all strains

Model		AICM(SE)
Clock model	Strict clock	8684.979(±0.204)
	Uncorrelated lognormal relaxed clock	**8648.535(±0.525)**
	Uncorrelated exponential relaxed clock	8657.437(±0.268)
	Random local clock	8687.156(±0.330)
Demographic model	**Constant size**	**8648.535(±0.453)**
	Exponential growth	8728.746(±0.248)
	Logistic growth	8707.971(±0.302)
	Expansion growth	8769.86(±0.454)

b) BA9 strains

Model		AICM(SE)
Clock model	Strict clock	3600.528(±0.193)
	Uncorrelated lognormal relaxed clock	3623.755(±0.232)
	Uncorrelated exponential relaxed clock	**3587.826(±0.436)**
	Random local clock	3601.761(±0.216)
Demographic model	Constant size	3587.826(±0.289)
	Exponential growth	**3573.785(±0.156)**
	Logistic growth	3576.116(±0.269)
	Expansion growth	3638.989(±0.241)

c) BA10 strains

Model		AICM(SE)
Clock model	Strict clock	3358.15(±0.175)
	Uncorrelated lognormal relaxed clock	3354.243(±0.104)
	Uncorrelated exponential relaxed clock	3346.371(±0.151)
	Random local clock	**3327.787(±0.07)**
Demographic model	Constant size	3327.787(±0.083)
	Exponential growth	3309.991(±0.056)
	Logistic growth	**3307.124(±0.066)**
	Expansion growth	3311.448(±0.076)

The selected models are indicated in bold letters.

Table 3. Models comparison based on AICM for Bayesian skyline plot

a) all BA strains

Model		AICM(SE)
Clock model	**Strict clock**	**6857.103(±0.495)**
	Uncorrelated lognormal relaxed clock	6962.146(±0.709)
	Uncorrelated exponential relaxed clock	6908.475(±0.726)

b) BA9 strains

Model		AICM(SE)
Clock model	**Strict clock**	**3581.845(±0.346)**
	Uncorrelated lognormal relaxed clock	3632.655(±0.290)
	Uncorrelated exponential relaxed clock	3591.545(±0.338)

c) BA10 strains

Model		AICM(SE)
Clock model	**Strict clock**	**3284.458(±0.092)**
	Uncorrelated lognormal relaxed clock	3296.686(±0.141)
	Uncorrelated exponential relaxed clock	3323.498(±0.288)

The selected models are indicated in bold letters.

Table 4. Evolutionary rates and estimated divergence

Genotype	Mean rate (95% HPD) (substitution/site/year)	Branching year (95% HPD) (year)
BA9	4.77×10^{-3} ($3.27\text{-}6.39 \times 10^{-3}$)	1999 (1994-2003)
BA10	4.81×10^{-3} ($3.02\text{-}6.67 \times 10^{-3}$)	2001 (1997-2004)
All strains	4.88×10^{-3} ($3.97\text{-}5.83 \times 10^{-3}$)	1951 (1936-1962)

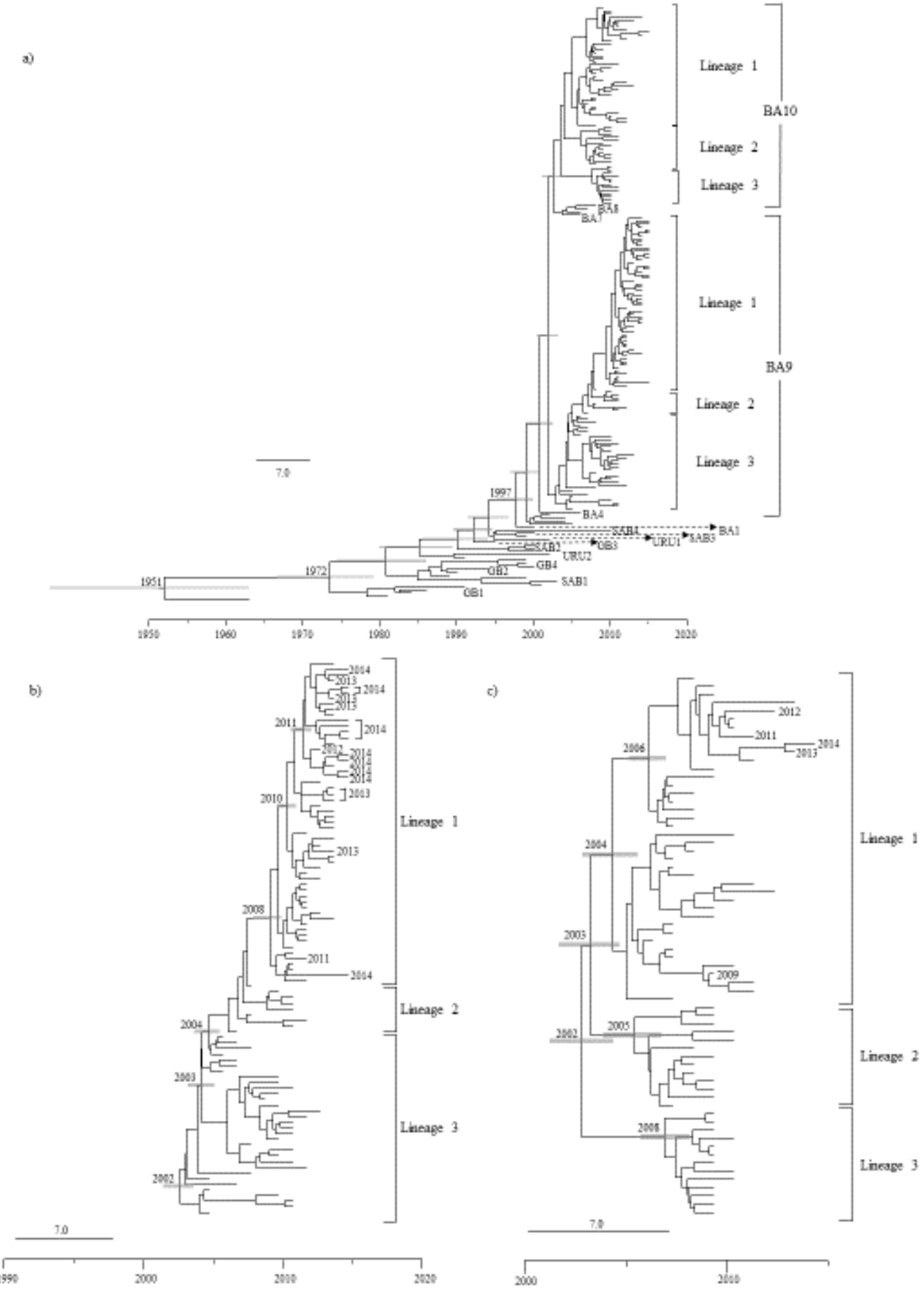

Figure 1. Phylogenetic trees for the *G* gene of HRSV-B (a), the expanded genotype BA9 (b), and the expanded genotype BA10 (c) constructed using the Bayesian Markov chain Monte Carlo method. Scale bars represent time (years). Gray bars indicate the 95% highest probability density (HPD) for the year of divergence. The Japanese strains detected during 2009-2014 is indicated by the year alone.

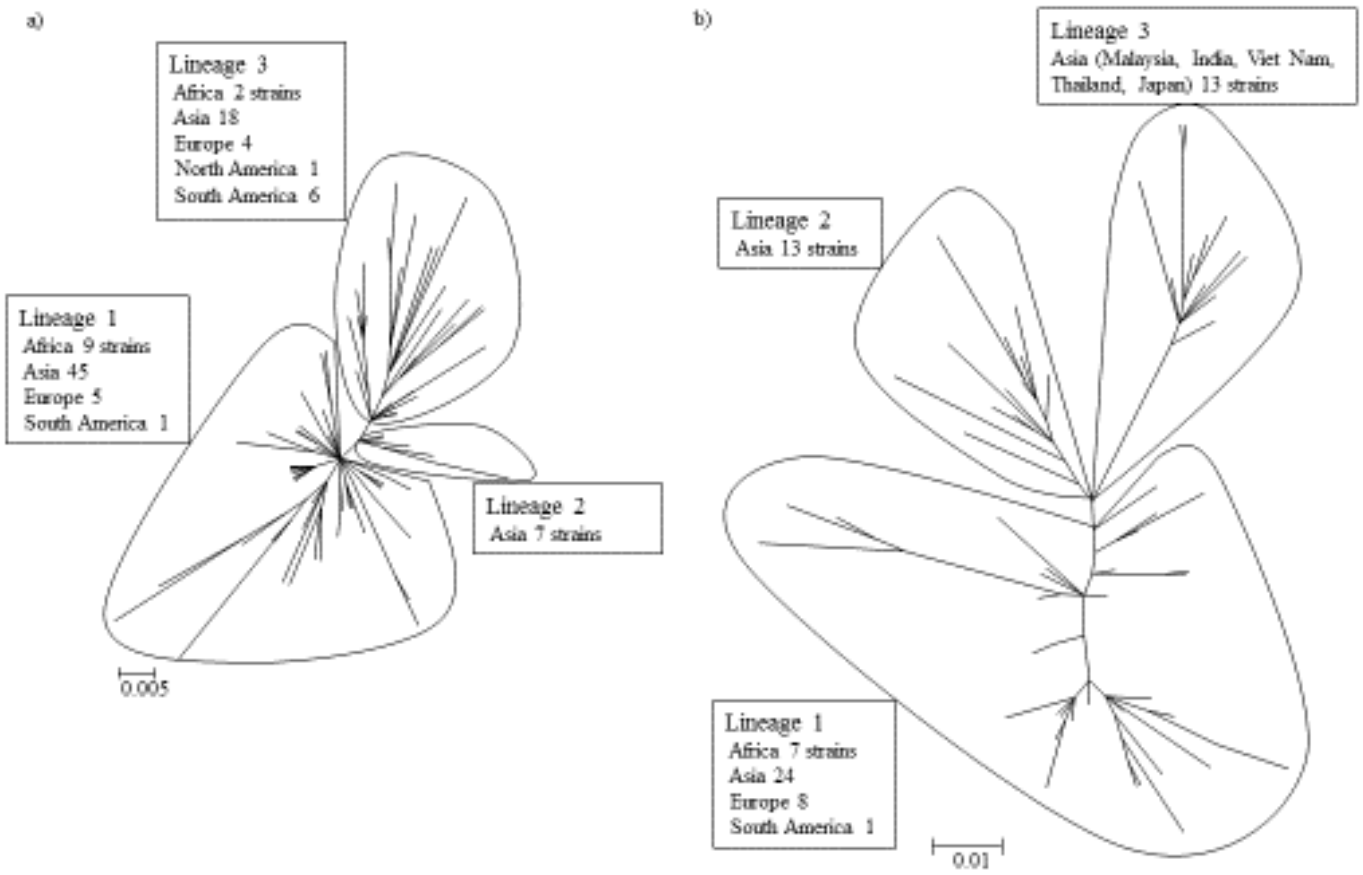

Figure 2. Phylogenetic tree for the *G* gene of HRSV-B genotype BA9 (a) and BA10 (b) constructed using the maximum likelihood (ML) method. Scale bar indicates nucleotide substitutions per site.

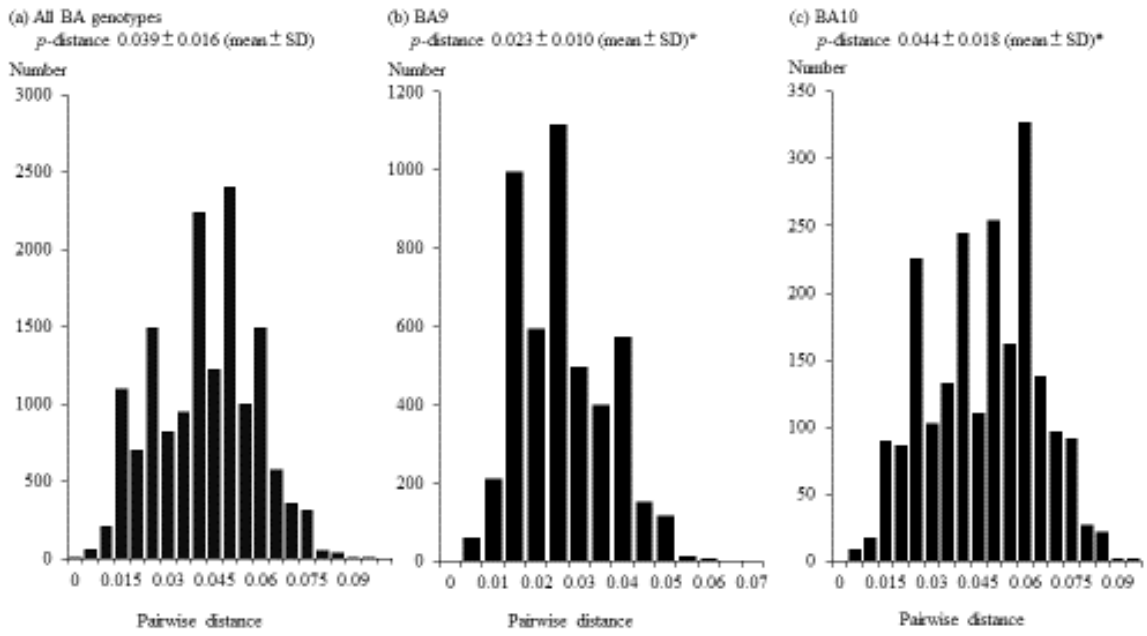

Figure 3. Distribution of pairwise distances (*p*-distances) between HRSV-B strains for all BA genotypes (a), genotype BA9 (b), and genotype BA10 (c) based on the nucleotide sequences of the *G* gene. * $p < 0.05$

Table 5. Sites exhibited positive selection in the C-terminal hypervariable region of the *G* gene

Genotype	Model	Positive selection site	mean dN/dS
All BA	SLAC	L219P, L219R, D253N, D253S, S267L, S267P, P267S, **Y287H**, **H287Y**	
	FEL	**Y287H**, **H287Y**	0.443
	IFEL	I270T, T270I, T270P, I270F, **Y287H**, **H287Y**	
BA9	SLAC	L219P, S267L, S267P, P267S	
	FEL	None	0.527
	IFEL	T250I, I270T, I270F, T270I, T270P, Y287H, H287Y	
BA10	SLAC	L219P, L219R	
	FEL	None	0.42
	IFEL	None	

Cut-off *p*-value < 0.05
The positive selection sites estimated by 3 methods are indicated in bold letters.

Table 6. Negative selection sites in C-terminal hyper variable region of G gene

Genotype	Model	Negative selection site
All BA	SLAC	**A220**, I229, V229, T250, **L252**, L272, P272, **H279**, **Q282**, **P291**, **L291**, **Q299**, **S304**, N310
	FEL	**A220,** P231, S231, T236, D243, S249, **L252**, T266, Q268, L272, P272, **H279**, **Q282**, **P291, L291**, P295, **Q299**, **S304**, S311
	IFEL	**A220**, S249, **L252**, **H279**, **Q282**, S285, **P291**, **L291**, P295, **Q299**, **S304**
BA9	SLAC	I229, **P295**, **S304**
	FEL	A220, P231, T239, L252, Q282, P291, L291, **P295**, **S304**, S307
	IFEL	**P295**, **S304**
BA10	SLAC	A220, T250, S269, P269, **L272**, H279, **P291**, **S304**, N310
	FEL	A220, S249,L252, **L272**, **P291**, P301, **S304**
	IFEL	L252, **L272**, **P291**, **S304**

Cut-off *p*-value < 0.05
The negative selection sites estimated by 3 methods are indicated in bold letters.

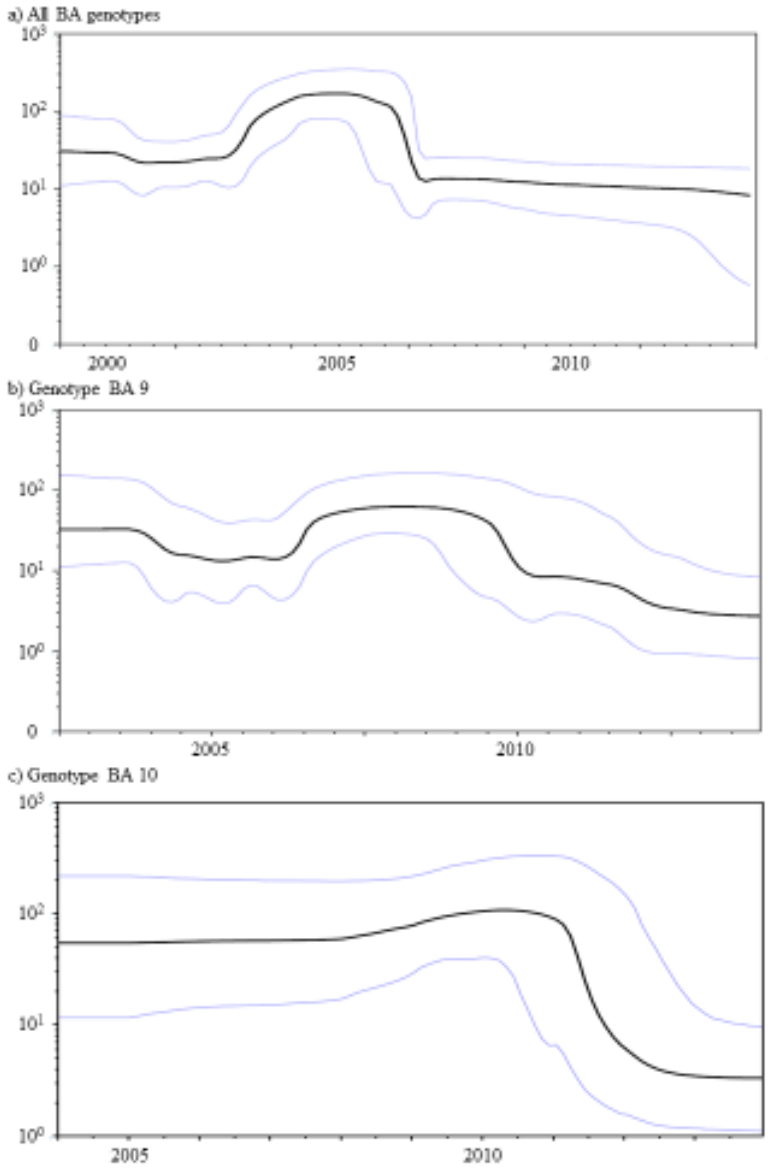

Figure 4. Phylodynamics of the *G* gene of HRSV-B for all BA genotypes (a), genotype BA9 (b), and genotype BA10 (c) using Bayesian skyline plot (BSP) analyses. The Y-axis shows the effective population size and the X-axis shows generation time (years). The black lines indicate mean effective population sizes and the gray lines indicate the 95% highest probability density (HPD).

Infection, Genetics and Evolution vol.36
平成 27 年 9 月 25 日　公表済